Research

New Phytologist

GLR-dependent calcium and electrical signals are not coupled to systemic, oxylipin-based wound-induced gene expression in *Marchantia polymorpha*

Maite Sanmartín[1]*, Enrique Rojo[2]*, Andrzej Kurenda[3], Beatriz Larruy-García[2], Ángel M. Zamarreño[4], M. Otilia Delgadillo[2], Pavel Brito-Gutiérrez[1], José M. García-Mina[4], Edward E. Farmer[3] and Jose J. Sánchez-Serrano[2]

[1]Instituto de Biología Molecular y Celular de Plantas, Universitat Politècnica de València, Consejo Superior de Investigaciones Científicas, Valencia, 46022, Spain; [2]Plant Molecular Genetics Department, Centro Nacional de Biotecnología-Consejo Superior de Investigaciones Científicas, Madrid, 28049, Spain; [3]Department of Plant Molecular Biology, University of Lausanne, 1015, Lausanne, Switzerland; [4]Department of Environmental Biology, Bioma Institute, University of Navarra, Pamplona, 31008, Spain

Author for correspondence:
Jose J. Sánchez-Serrano
Email: jjss@cnb.csic.es

Received: *29 December 2023*
Accepted: *18 April 2024*

New Phytologist (2024) **244:** 870–882
doi: 10.1111/nph.19803

Key words: calcium signalling, *Marchantia*, oxylipins, slow wave potentials, vasculature, wound.

Summary

- In angiosperms, wound-derived signals travel through the vasculature to systemically activate defence responses throughout the plant. In *Arabidopsis thaliana*, activity of vasculature-specific Clade 3 glutamate receptor-like (GLR) channels is required for the transmission of electrical signals and cytosolic Ca^{2+} ($[Ca^{2+}]_{cyt}$) waves from wounded leaves to distal tissues, triggering activation of oxylipin-dependent defences.
- Whether nonvascular plants mount systemic responses upon wounding remains unknown. To explore the evolution of systemic defence responses, we investigated electrical and calcium signalling in the nonvascular plant *Marchantia polymorpha*.
- We found that electrical signals and $[Ca^{2+}]_{cyt}$ waves are generated in response to mechanical wounding and propagated to nondamaged distal tissues in *M. polymorpha*. Functional analysis of Mp*GLR*, the only GLR encoded in the genome of *M. polymorpha*, indicates that its activity is necessary for the systemic transmission of wound-induced electrical signals and $[Ca^{2+}]_{cyt}$ waves, similar to vascular plants. However, spread of these signals is neither coupled to systemic accumulation of oxylipins nor to a transcriptional defence response in the distal tissues of wounded *M. polymorpha* plants.
- Our results suggest that lack of vasculature prevents translocation of additional signalling factors that, together with electrical signals and $[Ca^{2+}]_{cyt}$ waves, contribute to systemic activation of defences in tracheophytes.

Introduction

The evolution of a vascular system is one of the most crucial events that allowed plants to thrive and diversify in the early land environment (Delwiche & Cooper, 2015; de Vries & Archibald, 2018). Vasculature provided a sophisticated solution to a fundamental problem in the transition from the initial aqueous environment to the dry terrestrial habitats. The vascular system allowed plants to distribute water and minerals extracted from the soil and photoassimilates synthesised in aerial tissues for utilisation throughout the plant body. In addition, the thick cell walls of certain vascular tissues provided the required physical support for the increase in height and diversification in forms that tracheophytes (vascular plants) were to attain (Brodribb *et al.*, 2020; Woudenberg *et al.*, 2022). As an integral additional value, the vasculature provided a facilitated network for the rapid transmission of signals, chemical, electrical or otherwise, that permitted the coordination of actions throughout the plant in response to any local environmental stimuli (Hilleary & Gilroy, 2018). These achievements likely played an essential role in the establishment and expansion of plants in the terrestrial habitat, in which fluctuations in environmental conditions (light, temperature and humidity), and the subsequent appearance of novel pests and pathogens, would have posed tremendous pressures for land plant survival (Buatois *et al.*, 2022; Labandeira & Wappler, 2023).

Vascularisation, however, is not the only successful strategy in the conquest of land by plants. The diversification of the nonvascular bryophytes (hornworts, liverworts and mosses) and tracheophytes appears to have occurred early upon plant terrestrialisation (Kenrick & Crane, 1997; Wickett *et al.*, 2014; Morris *et al.*, 2018; Puttick *et al.*, 2018; Harris *et al.*, 2022). Comparative studies in bryophytes and tracheophytes are revealing, at a high level of detail, the changes in physiological processes and signalling networks that accompanied the establishment and subsequent expansion of land plants (Bowman *et al.*, 2017; Donoghue *et al.*, 2021;

*These authors contributed equally to this work.

Bowman, 2022). In this effort, the liverwort *Marchantia polymorpha* has been developed into a model system of choice (Shimamura, 2016; Bowman *et al.*, 2017, 2022; Kohchi *et al.*, 2021), as its responses to environmental stresses, and the underlying molecular pathways are similar to those present in tracheophytes (Bowman *et al.*, 2017; Monte *et al.*, 2018; Gimenez-Ibañez *et al.*, 2019). In addition, being nonvascular, *M. polymorpha* is an excellent system to study the evolution of long-distance signalling, in comparison with the mechanisms that have been identified in vascular plants.

Since the pioneering work in CA Ryan's laboratory (Green & Ryan, 1972), research done over the years in several laboratories in *Arabidopsis thaliana* and many other vascular plant species has shown that mechanical damage, such as that caused by wounding or insect feeding, triggers a response that is accompanied by a rapid and substantial reprogramming of gene expression (Delessert *et al.*, 2004; Kilian *et al.*, 2007). Importantly, this strong activation and repression of hundreds of wound-responsive genes is not restricted to the damaged tissue but also occurs in the distal, nondamaged parts (Titarenko *et al.*, 1997; Mousavi *et al.*, 2013). This response involves the accumulation of oxylipins, either through synthesis *in situ* and/or transport from wound sites, which then triggers an evolutionary conserved signal transduction pathway that mediates transcriptional reprogramming and defence gene activation in both locally damaged and distal intact tissues (León *et al.*, 2001; Schilmiller & Howe, 2005). A key component of this oxylipin signalling pathway, conserved in all land plants analysed, is the JAZ family of repressors, which are themselves also well-established markers of the transcriptional wound response (Chini *et al.*, 2007, 2009; Thines *et al.*, 2007; Browse, 2009; Monte *et al.*, 2018, 2019).

Comprehensive work, mostly done in *A. thaliana*, has conclusively established that this systemic wound response depends on a combination of signals, both chemical and electrical, that travel through the vasculature. Slow wave potentials (SWPs, also known as variation potentials) are electrical signals that underlie systemic activation of wound responses in vascular plants (Farmer *et al.*, 2020). These electrical signals are accompanied by transient increases in free cytosolic Ca^{2+} ($[Ca^{2+}]_{cyt}$) that move as a wave accompanying the variations in membrane potential. In addition, recent work revealed different chemical elicitors required for the systemic response to wounding (Gao *et al.*, 2023). Moreover, it has been unequivocally shown that Clade 3 glutamate receptor-like (GLR) channels are a fundamental component of this signalling pathway whose activity sustains both SWPs and $[Ca^{2+}]_{cyt}$ transients (Mousavi *et al.*, 2013; Nguyen *et al.*, 2018; Toyota *et al.*, 2018). The localisation of GLR3.3 and GLR3.6, the critical proteins involved in the long-distance transmission of the wound signals, is associated with the vascular tissue. Indeed, GLR3.3 localises principally to phloem sieve elements, whereas GLR3.6 protein levels are highest in the xylem contact cells (Nguyen *et al.*, 2018), supporting the crucial role of the vasculature in long-distance signalling. Analysis of the *M. polymorpha* genome sequence indicates that this liverwort has a single gene encoding a GLR (Mp*GLR*), most similar to *A. thaliana* Clade 3 *GLR*s, which is considered the most ancient clade (De Bortoli *et al.*, 2016).

In the present work, we wanted to elucidate the role of Mp*GLR* in the response to wounding, as well as any other function it may play in the physiology and development of *M. polymorpha*. Moreover, we wanted to ascertain whether a systemic response occurs in this nonvascular bryophyte in response to wounding and, if so, whether Mp*GLR* was part of the signalling network, as is the case in vascular plants. Our data indicate that calcium waves and electrical signals are part of an ancient, conserved wound signalling mechanism, modulated by GLR activity, which is transmitted systemically. However, the oxylipin-based gene regulatory response activated in wounded tissues is not coupled to this signalling activity in systemic tissues of *M. polymorpha*, suggesting that translocation of additional signalling components through the vasculature is essential for a proper reprograming of gene expression at distal tissues.

Materials and Methods

Growth conditions and plant transformation

Marchantia polymorpha L. accession Takaragaike-1 (Tak-1; male) was used as wild-type (WT) plant. Plants were grown on half-strength Gamborg's B5 medium containing 1% agar or in soil under a 16 h : 8 h, 22–24°C, light : dark photoperiod and relative humidity between 50% and 70%. *M. polymorpha* transgenic lines were generated using *Agrobacterium*-mediated transformation of regenerating thalli (Kubota *et al.*, 2013) and selected either on hygromycin or chlorsulfuron. Regenerated transgenic lines (T1) were initially characterised, and representative lines were further analysed. Asexual propagation (G1 gemmae) was used to maintain transgenic lines. Wounding was performed by crushing thallus lobes with a serrated forceps, damaging *c.* 40% of the surface (wounded tissues) while the adjacent lobes were collected as distal, nondamaged tissue (systemic tissues), as depicted schematically in Supporting Information Fig. S1.

Constructs

All primers used in this study are listed in Table S1. GCaMP3 sensor (Tian *et al.*, 2009) cloned at pDONR_Zeo (Invitrogen) was transferred to the binary vector pMpGWB110 to generate the construct Mp*EFpro::GCaMP3*. *Marchantia* Mp*GLR* (*Mp1g01040*) promoter and coding sequences were PCR amplified (Phusion® High-Fidelity; Thermo Fisher Scientific, Carlsbad, CA, USA) and cloned into pDONR207 vector for Gateway recombination-based subcloning (Invitrogen). For promoter analysis, the 4-kb upstream regulatory region and the first 63 bp of the Mp*GLR* coding sequence were PCR amplified and transferred to the destination vector pMpGWB104 (Ishizaki *et al.*, 2015), and transformed in regenerating Tak-1 thalli.

For transient expression, Mp*GLR* coding sequence in the pDONR207 vector was transferred to the destination vector pGWB5 (Nakagawa *et al.*, 2007) to generate a *35Spro*::Mp*GLR-GFP* construct. Agroinfiltration of *Nicotiana benthamiana* leaves was performed as described previously (Sanmartín *et al.*, 2011). To determine subcellular localisation, the endoplasmic reticulum

(ER) marker RFP-KDEL, the Multi-Vesicular-Body/Pre-Vacuolar Body compartment (MVB/PVC) marker RFP-ARA7, the Trans-Golgi Network (TGN) marker RFP-SYP61 and a Golgi localisation marker stTMD-RFP (Delgadillo *et al.*, 2020) were used for co-localisation analysis.

Generation of Mp*glr* mutants

To generate CRISPR-Cas9D10A nickase-mediated Mp*glr* mutants, four gRNAs, two targeting the first exon and two the second exon of the Mp*GLR* gene (Fig. S2), were cloned respectively into the pMpGE_EN04, pBC-GE12, pBC-GE23 and pBC-GE34 vectors. *Bgl*I digested fragments were subcloned into the pMpGE_EN04 and transferred to the pMpGE018 binary vector carrying the CRISPRCas9D10A nickase using LR Gateway reaction. Genomic DNA from G1 plants was amplified by PCR with primers listed in Table S1 and fragments sequenced to identify deletions. Stable genome editing was confirmed in G2 plants.

Confocal imaging

For confocal imaging, *N. benthamiana* samples were monitored using a Leica Stellaris 8 laser scanning confocal microscope (Leica Microsystems, Wetzlar, Germany). Excitation and emission wavelengths for GFP fluorescence were 514 nm and 517–554 nm, respectively, and for RFP, 561 and 598–658 nm, respectively. Images were captured by line sequential scanning to avoid signal bleed-through and minimise organelle displacement between captures.

Histochemical GUS assay

For β-Glucuronidase (GUS) assay, Mp*GLRpro::GUS* plants were incubated in GUS staining solution (100 mM sodium phosphate buffer pH 7.2, 0.5 mM $K_3Fe(CN)_6$, 0.5 mM $K_4Fe(CN)_6$, 1% Triton X-100 and 1 mg ml^{-1} 5-bromo-4-chloro-3-indolyl-β-D-glucuronic acid) at 37°C in the dark for 3 h. GUS-stained samples were cleared with ethanol and imaged with a Leica DMS 1000 stereoscopic or a Leica DM5000 microscope (Leica Microsystems). For histological analyses, GUS-stained thalli were dehydrated in ethanol, embedded in HistoResin and cut into 15-µm-thick sections. Eosin was used as a contrasting stain.

GCaMP3 fluorescence visualisation and quantification

Calcium imaging was performed as described previously (Nguyen *et al.*, 2018; Kurenda *et al.*, 2019). For that, an SMZ18 stereomicroscope (Nikon Instruments Europe BV, Amsterdam, the Netherlands) equipped with an ORCA-Flash4.0 (C11440) camera (Hamamatsu, Solothurn, Switzerland) and eGFP emission/excitation filter set (AHF Analysentechnik AG, Tübingen, Germany) was used. For quantification analysis, fluorescence measurements were defined in an area of 10 × 10 pixels located near electrode. Data processing was performed using MATLAB (MathWorks, Natick, MA, USA). Each experiment was replicated a minimum of four times.

Surface potential monitoring

Surface potentials were monitored as described previously (Nguyen *et al.*, 2018; Kurenda *et al.*, 2019). Surface electrodes were placed on the thallus, and a reference electrode of the same type was placed in the soil. Surface potential recordings were acquired at 100 Hz using the LABSCRIBE3 (iWorx Systems Inc., Dover, NH, USA) software. Data were analysed using custom-written scripts in MATLAB (MathWorks).

Total RNA extraction, qRT-PCR assays and transcriptome analyses

RNA was extracted and purified with Plant Total RNA Purification Kit (Favorgen, Ping Tung, Taiwan), including DNAse I digestion to remove any genomic DNA contamination. For gene expression analysis by quantitative reverse transcription polymerase chain reaction, cDNA was synthesised from 1 µg total RNA with the High-Capacity cDNA Reverse Transcription Kit (Thermo Fischer Scientific). Quantitative reverse transcription polymerase chain reaction was performed with PyroTaq EvaGreen qPCR Master Mix (ROX) 5X (Cultek Molecular Bioline, Madrid, Spain) and specific gene primers (Table S1), using 96-well or 384-well optical plates in 7500 HT or QUANTSTUDIO 5 Real-Time PCR systems (Thermo Fischer Scientific) with standard thermocycler conditions. For whole transcriptome analyses by RNA-Seq, three independent biological replicates per sample were sequenced. Each biological replicate consisted on RNA extracted from a pool of eight or nine plants from a given genotype and a given treatment. RNA samples were sent to Novogene or BGI Genomics and, after library preparation, sequenced with the Illumina NovaSeq 6000 S4 flowcell and DNBSEQ (DNBSEQ Technology, MGI, Shenzhen, China) platforms. For Microarray analysis, a custom *Marchantia* microarray (Agilent-084032 Marchantia_V1) was used, as described previously (Monte *et al.*, 2018). Two independent biological replicates per sample, each consisting of RNA extracted from a pool of 10 plants of a given genotype and treatment, were processed and hybridised with the microarrays. Two-Color Microarray-Based Gene Expression Analysis Protocol (Agilent Technologies, Santa Clara, CA, USA) was used to amplify and label RNA. Arrays were performed and analysed according to the manufacturer's instructions.

Oxylipin determination

Oxylipin measurements were performed as described previously (Kneeshaw *et al.*, 2022; Chini *et al.*, 2023) using three independent biological replicates per sample. Each sample contains tissue pooled from four plants. Data are shown as mean ± SD.

Results

Mechanical damage triggers systemic changes in surface potential and Ca^{2+} transients in *M. polymorpha*

In the liverwort *M. polymorpha*, different stimuli have been shown to cause local alterations in membrane potential that could

eventually spread as electrical signals to other parts of the plant (Kupisz *et al.*, 2017; Koselski *et al.*, 2021; Kisnieriene *et al.*, 2022). We wanted to determine whether, upon wounding of the thallus, this bryophyte, devoid of a vascular system, was able to sustain and propagate electrical signals, reaching nondamaged distal tissues. To this end, an electrode was applied to the thallus surface of 6-wk-old, soil-grown *M. polymorpha* plants, at the edge of a thallus lobe, while the adjacent lobe was wounded by crushing once with a serrated forceps. A few seconds after mechanical damage, a change in surface potential was recorded at the distal, nondamaged part of the thallus (Fig. 1a; Video S1) that resembled the SWPs that transmit wound signals in vascular plants.

In *A. thaliana* and other vascular plants, SWPs are accompanied by transient increases in cytosolic Ca^{2+} concentration ($[Ca^{2+}]_{cyt}$) that spread to distal tissues. To monitor $[Ca^{2+}]_{cyt}$, we generated transgenic *M. polymorpha* lines expressing the GCaMP3 fluorescent sensor (Tian *et al.*, 2009) under the control of the constitutive elongation factor 1α (Mp*EF1α*) promoter (Althoff *et al.*, 2014; Mp*EFpro::GCaMP3*). We obtained over 50 independent Mp*EFpro::GCaMP3* transgenic lines, all showing qualitatively similar fluorescence levels in control conditions and in response to wounding. Moreover, the constitutive expression of the Ca^{2+} sensor did not confer any obvious phenotype to the transgenic plants under standard growth conditions. Two independent Mp*EFpro::GCaMP3* expressing lines (L47 and L48) were chosen for further characterisation. L47 and L48 plants were wounded and variations in $[Ca^{2+}]_{cyt}$ monitored. A surface electrode applied to the plants to be wounded, permitted the simultaneous recording of membrane depolarisations and $[Ca^{2+}]_{cyt}$ transients.

Changes of surface potential after wounding were similar to those recorded in WT Tak-1 plants (Fig. 1a; Video S2). Before wounding, only gemmae cups and apical notches showed detectable fluorescence, either due to high Ca^{2+} levels and/or higher activity of the Mp*EF1α* promoter (Fig. 1b,c). Wounding the apical part of a thallus lobe resulted in transient increases of $[Ca^{2+}]_{cyt}$, monitored as an increase in the fluorescence emitted by the GCaMP3 sensor (Fig. 1b,c; Video S2). A fluorescence wave could be observed moving through the thallus (Videos S2, S3). As the wave passed, particularly high fluorescence was detected in gemmae cups, and at the apical notches. $[Ca^{2+}]_{cyt}$ also increased transiently at the lobes of distal thalli, with maximal fluorescence being also displayed at gemmae cups and apical notches (Fig. 1c; Video S3). This fluorescence wave appeared to move uniformly along the thallus. Remarkably, at distal tissues, the highest level of fluorescence (the wavefront) was attained with some delay after the variation in surface potential had reached the position where the electrode was placed, during the initial stages of the recovery (repolarisation) phase (Video S2).

Wound-induced surface potential variations and $[Ca^{2+}]_{cyt}$ transients depend on GLR activity

In *A. thaliana*, wound-induced SWPs and $[Ca^{2+}]_{cyt}$ transients are abolished in the *glr3.3 glr3.6* double mutant (Mousavi *et al.*, 2013; Nguyen *et al.*, 2018; Toyota *et al.*, 2018). We wanted to determine whether the wound-induced membrane potential changes and $[Ca^{2+}]_{cyt}$ transients observed in *M. polymorpha* are, as in vascular plants, dependent on GLR activity. Analysis of the *M. polymorpha* genome revealed the presence of a single GLR gene (*Mp1g01040*/Mp*GLR*). The functional characterisation of Mp*GLR* was undertaken using a CRISPR-Cas-based approach to generate Mp*glr* mutant alleles in the L47 and L48 backgrounds. Two independent, putative knock-out alleles were further characterised, Mp*glr-7* and Mp*glr-9* (Fig. S2). The Mp*glr-7* allele generated in the L47 background has a deletion that alters the reading frame of the resulting transcript, introducing a premature stop codon. The transcript produced would only code for the first 36 amino acids of the protein, lacking the domains involved in ligand binding and channel activity. Moreover, Mp*GLR* transcript levels are strongly reduced in Mp*glr-7* plants (Fig. S2), probably due to degradation through the nonsense-mediated decay pathway. All considered, it is most likely that Mp*glr-7* is a null allele. The second allele Mp*glr-9* was generated in the L48 background and has a deletion that produces a truncated transcript, which maintains the reading frame but eliminates 139 amino acids from the amino-terminal domain of the protein involved in channel regulation (Wudick *et al.*, 2018; Yan *et al.*, 2024; Fig. S2). Mp*GLR* transcript levels were not significantly altered in the Mp*glr-9* allele (Fig. S2), suggesting that this deletion has no effect on transcript stability. Mp*glr-7* and Mp*glr-9* plants were indistinguishable from the L47 and L48 parental lines when grown *in vitro* or in soil (Fig. S3), indicating that MpGLR activity is not required for normal vegetative growth and development. Interestingly, electrical signals and transient $[Ca^{2+}]_{cyt}$ increases detected in the distal nondamaged tissues of wounded plants with the WT Mp*GLR* (Tak-1, L47 and L48 lines) were largely abolished in both Mp*glr* mutant lines (Figs 2, S4; Videos S2, S4). These results strongly support the involvement of MpGLR activity in the generation and/or systemic transmission of changes in surface potentials and $[Ca^{2+}]_{cyt}$ transients upon wounding.

Mp*GLR* is expressed at the midrib and localises to the ER and multivesicular bodies

In *A. thaliana*, the most abundant GLR3.3 and GLR3.6 protein pools localise to phloem sieve elements and xylem contact cells, respectively (Nguyen *et al.*, 2018), consistent with the essential role of the vasculature in the transmission of wound signals in this species. We wondered whether Mp*GLR* would also have a certain level of domain-specific expression within the thallus. To investigate Mp*GLR* expression with spatial resolution, we generated a construct consisting of a 4-kb promoter fragment upstream of the translation start site, fused to the *GUS* reporter gene (Mp*GLRpro::GUS*). We transformed *M. polymorpha* plants and generated over 35 independent Mp*GLRpro::GUS* transgenic lines. All GUS-positive lines obtained had a similar activity pattern, characterised by maximal GUS activity at the central zone of the thallus encompassing the midrib, and being essentially undetectable at the thallus margins (Fig. 3a,b). Cross-sections of

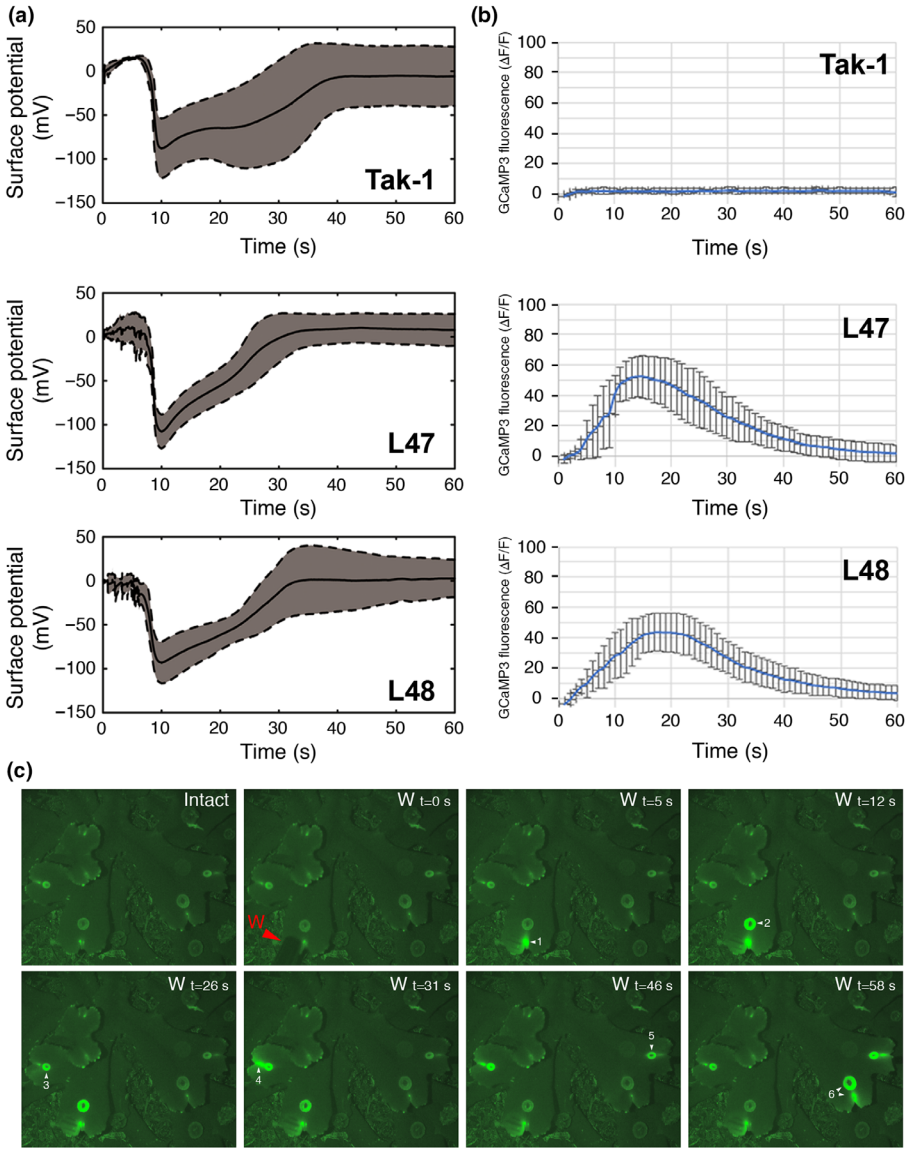

Fig. 1 Systemic membrane depolarisation and Ca^{2+} transients are triggered in *Marchantia polymorpha* in response to wounding. (a) Systemic surface potential changes in 6-wk-old, mechanically wounded *M. polymorpha* thalli from Tak-1 and L47 and L48 GCaMP3 expressing lines, grown on soil. A thallus lobe was wounded while the recording electrode was placed in the adjacent, nondamaged lobe (lines are the average of n = 5–10 plants per genotype; envelopes ±SD). (b) Systemic GCaMP3 fluorescence monitoring. Averaged ±SD fluorescence adjusted according to time of wounding (t = 0; n = 5–10 plants per genotype). Fluorescence was measured in the apical notch of the adjacent, nondamaged lobe. (c) Representative pictures showing GCaMP3 fluorescence in *M. polymorpha* L47 thalli before (intact) and after wounding (W) a lobe with forceps (red arrowhead). Time points after wounding are shown at the top right of each panel. Numbers 1–6 indicate the gradual transmission of a calcium wave to lobes progressively further from the wound site. Frames are taken from Supporting Information Video S3.

the Mp*GLRpro::GUS* thallus showed GUS activity in all tissue layers at the centre of the thallus, including dorsal and ventral epidermis, air chambers, parenchyma tissue and rhizoids (Fig. 3b). Isolated spots of high GUS activity are also observed that likely correspond to oil cells (Shimamura, 2016).

To determine the subcellular distribution of the MpGLR, we expressed a C-terminal GFP fusion to MpGLR (MpGLR-GFP) in *N. benthamiana* and analysed the localisation by confocal microscopy. MpGLR-GFP fluorescence was found primarily at the ER co-localising with RFP-KDEL (Fig. 3c), but also labelled punctate structures (marked by arrowheads in Fig. 3c), which likely represent an endosomal compartment. To determine the nature of that compartment, we co-expressed MpGLR-GFP with the Golgi marker STtmd-RFP, the TGN marker RFP-SYP61 and the MVB/PVC marker RFP-ARA7 (Delgadillo *et al.*, 2020). A clear co-localisation of MpGLR-GFP and RFP-ARA7 in the punctate structures was observed, whereas no co-localisation was observed with Golgi or TGN markers (Fig. 3c). These results show that the most abundant detectable pools of MpGLR-GFP are located at the ER and MVB/PVCs in *N. benthamiana* cells. These experiments do not rule out the presence of as yet undetected MpGLR pools in the plasma membrane. However, the localisation of MpGLR to the ER is consistent with that reported for AtGLR3.3 (Nguyen *et al.*, 2018) and the likely localisation of AtGLR1.2, AtGLR1.3 (Zheng *et al.*, 2018) and AtGLR3.7 (Wang *et al.*, 2019). This conserved localisation of orthologues from distant plant families suggests that the ancestral GLR was ER-localised.

Damage-induced gene expression is restricted to the vicinity of the wound and is MpGLR-independent

In vascular plants, wounding leads to a substantial reprogramming of gene expression both in the damaged tissue and in distal,

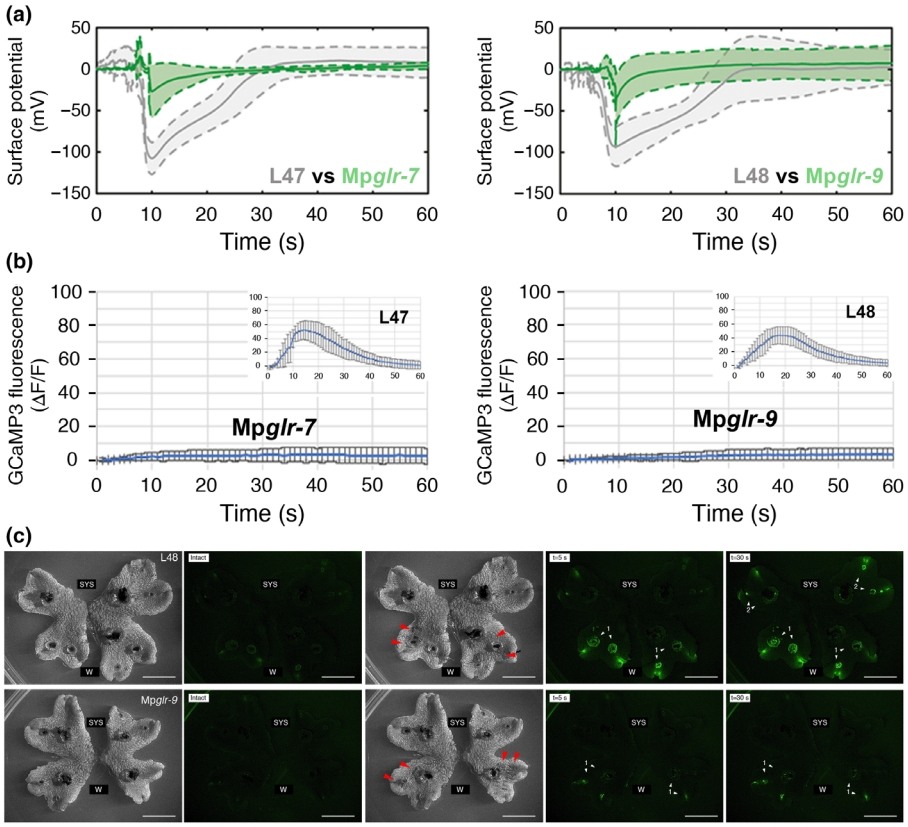

Fig. 2 Systemic wound-induced surface potentials and cytosolic Ca^{2+} ($[Ca^{2+}]_{cyt}$) transients in wild-type (WT) and Mp*glr* mutant plants. (a) *Marchantia polymorpha* carrying the GCaMP3 Ca^{2+} sensor (L47 and L48; grey lines) and the Mp*glr* mutant lines (green lines) were wounded at the thallus and surface potentials recorded from an electrode placed in the adjacent, nondamaged lobe. Average graphs ±SD envelopes are shown for each line. (b) Average increases in GCaMP3 fluorescence upon wounding of Mp*glr* mutant lines. Fluorescence was measured in the apical notch of the adjacent, nondamaged lobe. Inset shows GCaMP3 fluorescence changes in *Marchantia* L47 and L48 lines. Averaged ±SD fluorescence adjusted according to time of wounding (t = 0; n = 5–10 plants per genotype). (c) Representative images of GCaMP3 fluorescence in L48 and Mp*glr-9* plants grown *in vitro*, before (intact) and after wounding plants with a serrated forceps (red arrowheads). The wounded lobes (W) and distal nondamaged (SYS) lobes are indicated. Time points after wounding are shown at the top left of each panel. $[Ca^{2+}]_{cyt}$ spikes in damaged lobes (1) and systemic lobes (2) are indicated with white arrowheads. Bars, 0.5 cm.

nondamaged parts of the plant. Recently, a genome-wide study uncovered a large number of wound-regulated genes in the damaged tissue of *M. polymorpha* (Monte *et al.*, 2018; Liang *et al.*, 2022), but the expression in nondamaged tissues of the wounded plants was not analysed. To determine whether *M. polymorpha* plants activate a systemic gene response to wounding, and what role Mp*GLR* may play in this process, we performed RNA-Seq analysis on the Mp*glr* mutants and the corresponding L47 and L48 control lines, by separately analysing damaged tissues from distal, nondamaged ones (Fig. S1). We compared the wound response of WT and Mp*glr* mutant plants in two different conditions, in plants grown *in vitro*, as in the previously published study (Liang *et al.*, 2022), and in plants grown in soil, which more closely resembles a natural environment. After analysing by quantitative reverse transcription polymerase chain reaction, the expression of the well-established wound-responsive genes Mp*DIR*, Mp*AWI3* and Mp*JAZ* (Monte *et al.*, 2018, 2019; Liang *et al.*, 2022) at different time points, we chose 2 and 4 h after wounding, which displayed maximal wound induction levels, to capture both early and late gene expression changes by RNA-Seq.

At both time points, we observed a large transcriptional reprogramming in wounded tissues of control and Mp*glr* mutant lines. In soil-grown L47 plants, we found 980 genes strongly induced and 413 strongly repressed ($|\log_2$Fold-change$|$, $|\log_2 FC| > 1$, false discovery rate, FDR < 0.05) at the site of damage 2 h after wounding, relative to tissues from intact plants (Fig. 4a,b). Likewise, 912 genes were strongly induced and 622 were strongly repressed in damaged tissues of *in vitro*-grown L48 plants 4 h after wounding. The sets of differentially expressed genes after 2 h or 4 h of wounding in soil- or in *in vitro*-grown plants were highly overlapping, with 658 genes highly induced and 156 highly repressed in both conditions and time points (Fig. 4a). Moreover, virtually the same transcriptional response was observed in damaged tissues of Mp*glr* mutants (Fig. 4; Table S2), strongly supporting that Mp*GLR* is not involved in regulating local wound gene responses in *M. polymorpha*. For instance, all 980 strongly induced and 413 strongly repressed genes in wounded tissues of soil-grown L47 plants are also induced and repressed, respectively, in wounded tissues of Mp*glr-7* plants (Fig. 4b). Taken together, our RNA-Seq studies identified a set of 567 genes that are strongly induced in wounded tissues in all conditions, time points and genotypes tested (Fig. 4a). Gene Ontology analysis on this robust set of upregulated genes in damaged *M. polymorpha* tissues revealed an enrichment in terms such as oxylipin biosynthetic process, aromatic amino acid biosynthesis and metabolism, or response to wounding (Fig. 4c).

In contrast to the large-scale gene reprogramming observed in damaged tissues, very few significant differences in gene expression could be identified when the transcriptome of distal, intact tissues of wounded plants was compared with the nonwounded control plants, for both L47/L48 lines and the corresponding Mp*glr* mutants. In L48 or Mp*glr-9* plants grown *in vitro*, no differentially expressed genes (FDR < 0.05) were found when

New Phytologist

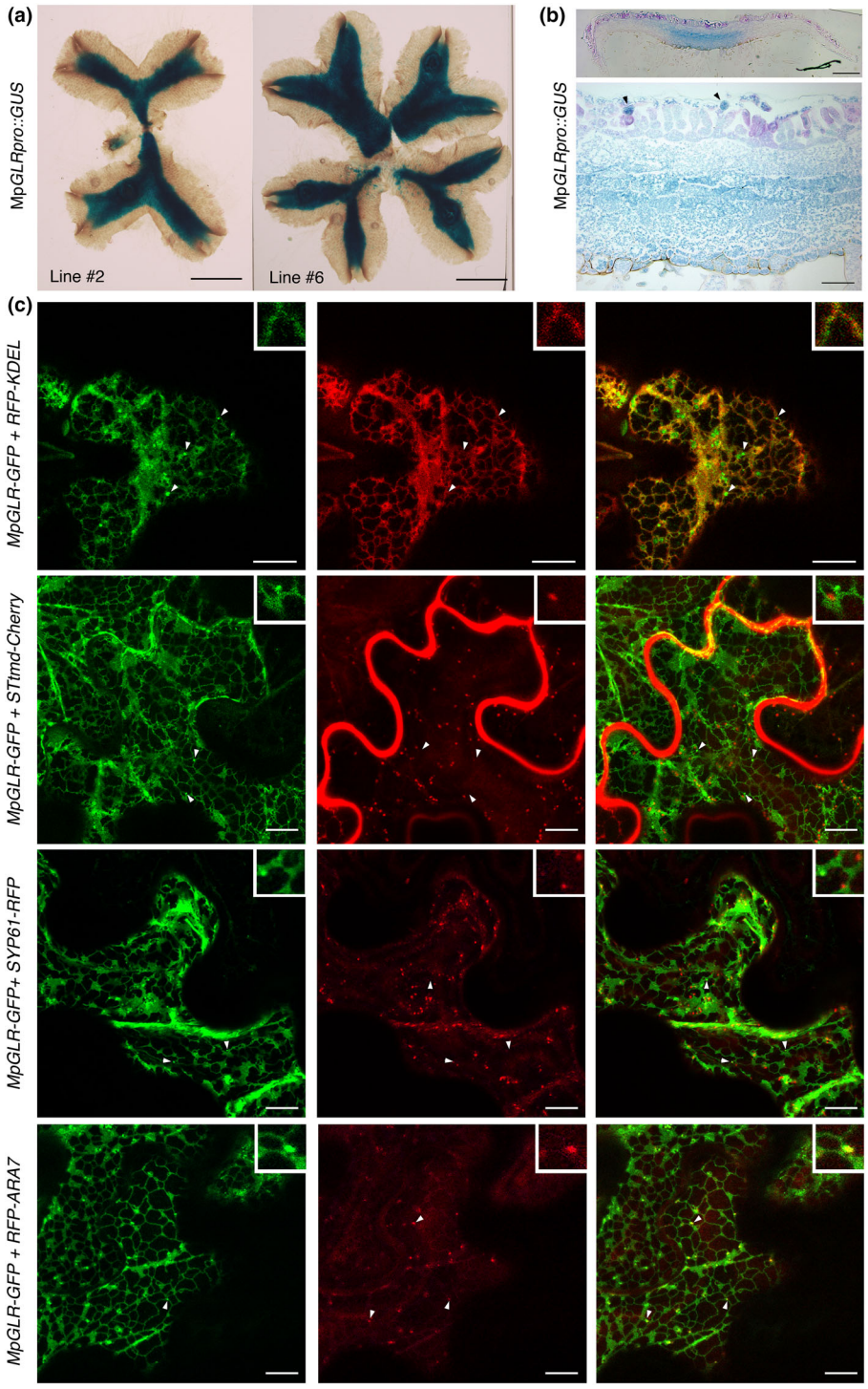

Fig. 3 Mp*GLR* is expressed along the midrib during the vegetative phase of *Marchantia polymorpha*. (a) Histological staining pattern of β-Glucuronidase (GUS) activity in 21-d-old plants from two Mp*GLRpro::GUS* representative lines. Bars, 0.5 cm. (b) Transversal cross-section close to the basal region of the thallus. Bars: (upper panel) 0.5 mm; (lower panel) 100 μm. Arrowheads indicate oil cells (c) Confocal images of *Nicotiana benthamiana* epidermal cells co-transformed with MpGLR-GFP and the endoplasmic reticulum (ER) marker RFP-KDEL, the Golgi marker STtmd-Cherry, the Trans-Golgi-Network (TGN) marker RFP-SYP61 or the Multi-Vesicular-Body (MVB) marker RFP-ARA7. Panels show the GFP signal (green pseudocolour), the RFP signal (red pseudocolour) and the merged image of both signals. Arrowheads indicate punctate structures labelled with MpGLR-GFP. Insets show a representative region. Bars, 10 μm.

comparing samples from intact plants to those from systemic, nondamaged tissues of plants 4 h after wounding. In plants grown in soil, 24 genes were strongly deregulated 2 h after wounding (FDR < 0.05, $|\log_2 FC| > 1$, 2 induced and 22 repressed) in systemic *vs* control tissues of L47 plants, whereas six genes were deregulated (one induced and five repressed) in Mp*glr-7* plants. However, none of the upregulated genes in systemic tissues was shared between the different samples. Moreover, of the core 567 genes induced in all conditions in damaged tissues, none were induced to any significant extent in systemic tissues (Fig. 4b; Table S2). Instead, only three genes were downregulated ($|\log_2 FC| > 1$) in systemic tissues in all genotypes (Fig. 4d), albeit not significantly (FDR > 0.8) in L48 and Mp*glr-9* plants (Table S2). These RNA-Seq results show that wounding causes a

global transcriptional reprogramming in damaged tissues but has virtually no effect on the transcriptome in systemic tissues under the experimental conditions used.

To exclude that the lack of systemic response was due to the presence of the GCaMP3 sensor in the genotypes analysed, we performed a transcriptomic analysis of wounded Tak-1 plants grown in soil (Table S3). In Tak-1, we found 1612 genes strongly deregulated (FDR < 0.05, $|\log_2 FC| > 1$, 923 induced and 689 repressed) in damaged tissues relative to intact plants while in systemic tissues there were only 19 differentially expressed genes (12 induced and 7 repressed). Moreover, none of the genes found to be deregulated in systemic tissues in Tak-1 coincided with those deregulated in L47 and Mp*glr-7* soil-grown plants, and none were found to be deregulated in L48 and Mp*glr-9 in vitro*-grown plants, indicating that their differential expression is not a conserved transcriptional response in systemic tissues.

To further substantiate these results, we analysed by quantitative reverse transcription polymerase chain reaction, the expression of Mp*DIR*, Mp*AWI3* and Mp*JAZ* in independent samples. In accordance with the lack of a systemic gene response observed in the whole-genome transcriptomic studies, no activation of these wound-responsive genes was detected in the distal, nondamaged tissues in control and Mp*glr* plants, 1, 2 or 24 h after wounding (Fig. 4e). Moreover, knocking out Mp*GLR* has little effect on wound-responsive gene expression at the damaged tissues (Fig. 4e). Together, these extensive transcriptional analyses show that, under our experimental conditions, there is no consistent systemic regulation of gene expression in wounded WT *M. polymorpha* plants. This lack of a systemic response is somewhat unexpected as changes in surface potentials and $[Ca^{2+}]_{cyt}$ transients indicate distribution of the wound signal throughout the plant body and are produced in *M. polymorpha* upon wounding. However, the absence of a wound response in distal tissues would largely fit with the fact that systemic spread of wound signals in *A. thaliana* occurs via the vasculature (Gao *et al.*, 2023), of which *M. polymorpha* is devoid.

Wound-induced synthesis of oxylipins is restricted to locally damaged tissues

Accumulation of oxylipins upon wounding in both damaged and distal tissues is fundamental to activate the transcriptional defence response (León *et al.*, 2001; Schilmiller & Howe, 2005). Interestingly, expression of genes implicated in the synthesis of dn-*iso*-OPDA, dn-*cis*-OPDA and Δ4-dn-*iso*-OPDA, which in *M. polymorpha* are the main ligands of the MpCOI1-MpJAZ receptor (Monte *et al.*, 2018; Kneeshaw *et al.*, 2022), is induced in damaged tissues in our experiments (Fig. 5a). This is the case in many, if not all, vascular plants where the response to wounding has been studied (Wasternack & Hause, 2013; Kimberlin *et al.*, 2022). We wanted to determine whether this increased expression of oxylipin biosynthetic genes is translated into higher levels of these compounds in wounded plants. To this end, an oxylipin profile of *M. polymorpha* thallus was obtained. Targeted metabolomic analyses revealed high increases in oxylipin compounds upon wounding in damaged tissues, including the signalling active dn-*iso*-OPDA, dn-*cis/trans*-OPDA and Δ4-dn--*iso*-OPDA (hereafter dn-OPDAs; Fig. 5b; Table S4). Moreover, levels of other OPDA-related molecules, including, *cis*-OPDA, *tn*-OPDA, C14-*iso*-OPDA and C20-OPDA, also increased in wounded tissues (Table S4). As expected, Mp*glr* mutants attained similar levels as those in WT plants (Fig. 5b; Table S4). In accordance to the lack of a systemic gene response in *M. polymorpha*, no significant increase in oxylipin levels was detected in the distal, nondamaged tissues of wounded WT or Mp*glr* plants (Fig. 5b; Table S4). These results also suggest that, within the time frame of the experiment, neither induced oxylipin synthesis in systemic tissues nor transport from the damaged tissue occurs in a significant manner in *M. polymorpha*.

Discussion

Plant terrestrialisation is undoubtedly one of the most fundamental steps for the evolution of life on Earth. It not only entailed the colonisation of a pristine habitat that enabled the expansion and diversification of plants but also permitted the simultaneous land expansion of the animal kingdom (Tihelka *et al.*, 2022), for which land plants provided an oxygen-rich atmosphere and the necessary nutritional resources (Labandeira & Wappler, 2023). The appearance of animals feeding on plants represented a new threat that likely drove the evolution of rapid and efficient defence signalling mechanisms. In this context, the acquisition of a vasculature offered a novel way to spread danger signals throughout the plant body allowing to mount faster and more effective defence responses. However, nonvascular liverworts similar to their extant relatives were widely distributed in the early time of land invasion (Wellman *et al.*, 2003; Hernick *et al.*, 2008), and probably represented an easy prey for the newly arrived plant feeders since most of their bodies develop close to the soil. However, the fact that bryophytes, liverworts among them, persisted and are abundant today indicates that the defence strategies of their extinct relatives did not pose a major disadvantage compared to the more evolved vascular-associated signalling.

Aiming to understand the evolution of wound signalling in plants, we have studied the responses to mechanical damage in the liverwort *M. polymorpha*, and compared our results to the model established for the vascular plant *A. thaliana*. We show that the response to wounding in *M. polymorpha* entails a reprogramming of gene expression that, in contrast to what occurs in vascular plants, is limited to the vicinity of the damaged tissue. Indeed, RNA-Seq analysis shows that upon damage many defence-related genes are activated, which are part of the protective response. Among other physiological processes, wound-induced activation of the oxylipin biosynthetic genes leads to a rapid increase in the concentration of dn-OPDAs (this work; Monte *et al.*, 2018; Kneeshaw *et al.*, 2022), the master wound-hormone regulators in *M. polymorpha* (Kneeshaw *et al.*, 2022; Chini *et al.*, 2023). Targeted metabolomic analysis has revealed that this increase in dn-OPDAs and related compounds occurs in the tissues close to the wound site but is not detected in distal

parts of the wounded thallus, thus again differing from vascular plants.

In *A. thaliana,* it has been established that wound-induced SWPs (monitored as variations in surface potentials) and $[Ca^{2+}]_{cyt}$ transient waves both depend on the activity of GLR channels (Mousavi *et al.*, 2013; Nguyen *et al.*, 2018; Toyota *et al.*, 2018). Several studies have shown that SWPs are transmitted via the vasculature from the site of damage to distal undamaged tissues, where they result in both increases in oxylipin synthesis and a large reprogramming of gene expression (Kurenda

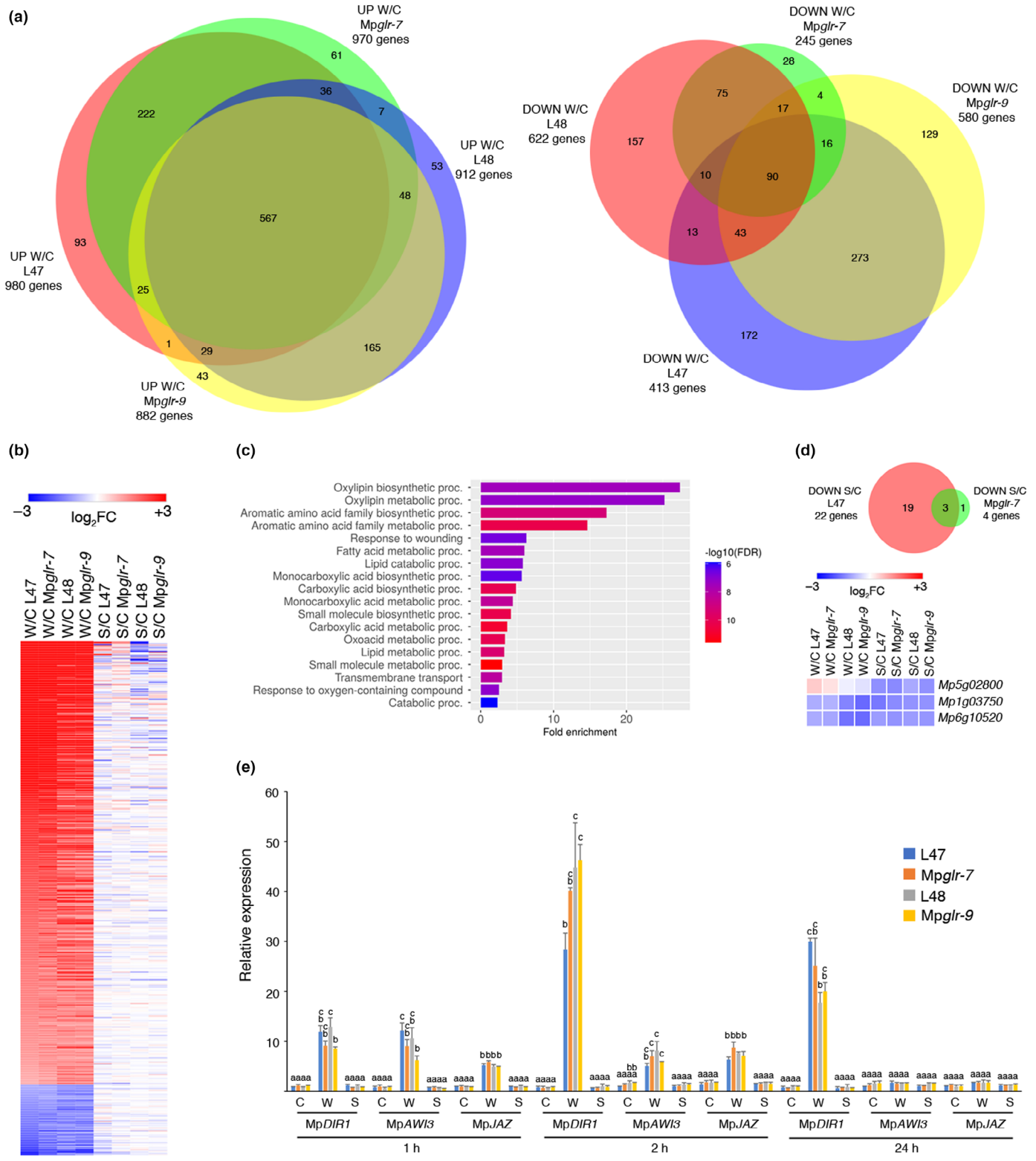

Fig. 4 Glutamate receptor-like (GLR) involvement in regulating wound-responsive gene expression in *Marchantia polymorpha*. (a) Venn diagram analysis of genes strongly (false discovery rate [FDR] < 0.05, $|\log_2 FC| > 1$) upregulated (left panel) and downregulated (right panel) after wounding relative to intact plants (W/C) in samples from L47 and Mp*glr-7* plants grown in soil 2 h after wounding and L48 and Mp*glr-9* plants grown *in vitro* 4 h after wounding. (b) Heat map showing $\log_2 FC$ gene expression in wounded tissues vs intact plants (W/C) or systemic tissues vs intact plants (S/C) of the overlapping 567 upregulated genes and 90 downregulated genes from the Venn diagram analysis in panel A. (c) Significant Gene Ontology (GO) terms (biological process) associated with 567 transcripts strongly induced (FDR < 0.05, $|\log_2 FC| > 1$) in all genotypes and time points analysed. GO terms correspond to the most similar genes in *Arabidopsis thaliana*. (d) Venn diagram analysis of genes strongly (FDR < 0.05, $|\log_2 FC| > 1$) downregulated in systemic tissues relative to intact plants (W/C) in samples from L47 and Mp*glr-7* plants grown in soil 2 h after wounding. Below, a heat map of $\log_2 FC$ gene expression in wounded tissues vs intact plants (W/C) or systemic tissues vs intact plants (S/C) of the overlapping three genes from the Venn diagram analysis above. (e) Quantitative reverse transcription polymerase chain reaction analysis of selected wound-responsive gene expression in intact plants (C) and in wounded tissues (W) and nondamaged systemic tissues (S) 1, 2 and 24 h after wounding in plants grown *in vitro*. The genotypes are indicated in the labels. Error bars represent SD ($n = 2$ independent samples). This experiment was repeated twice with similar results. ANOVA with Tukey's HSD *post hoc* test was used to test for differences among the means in each experimental time point. Means without letters in common are significantly different ($P < 0.05$).

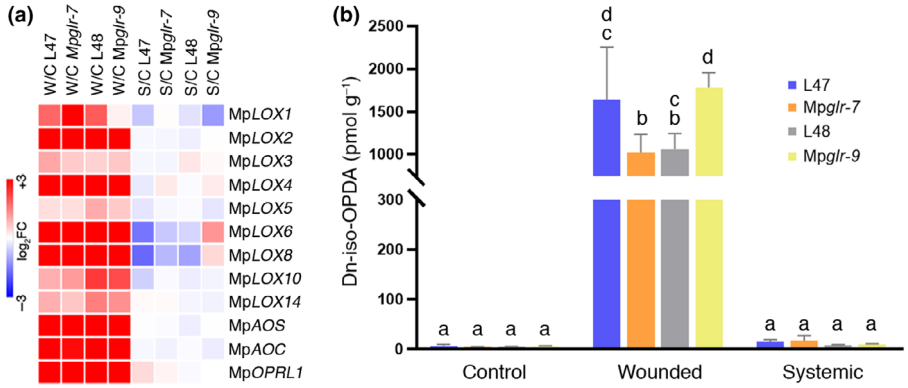

Fig. 5 Loss of Mp*GLR* has no effect in dn-*iso*-OPDA accumulation in damaged *Marchantia polymorpha* thalli. (a) Fold enrichment of transcripts involved in oxylipin biosynthesis in wound (W/C) and nondamaged distal tissues vs control conditions (S/C) in the different genotypes. (b) Accumulation of dn-*iso*-OPDA in control lines (L47 blue; L48 grey bars) and both Mp*glr* mutant lines (Mp*glr7*, orange; Mp*glr9*, yellow bars) in basal conditions, and 1 h after mechanical wounding in local (wounded) and distal nondamaged (systemic) tissues. Data are means ± SD ($n = 3$). ANOVA with Tukey's HSD *post hoc* test was used to test for differences among the means. Means without letters in common are significantly different ($P < 0.05$).

et al., 2019; Gao *et al.*, 2024). In the present work, we have indeed detected membrane depolarisations upon wounding of the *M. polymorpha* thallus, similar to the wound-induced SWPs described in *A. thaliana* (Mousavi *et al.*, 2013; Nguyen *et al.*, 2018). Introducing the GCaMP3 Ca^{2+} sensor has allowed us to simultaneously monitor alterations in $[Ca^{2+}]_{cyt}$. We have observed that $[Ca^{2+}]_{cyt}$ waves uniformly spread across the *M. polymorpha* thallus after wounding. In addition, we have generated GLR-deficient *M. polymorpha* lines by CRISPR-Cas-mediated deletion of the only Mp*GLR* gene. In the mutant plants, wound-induced electrical signals and $[Ca^{2+}]_{cyt}$ transients are essentially abolished, very much resembling what is observed in vascular plants. These results are in agreement with the recent report by Watanabe *et al.* (2024) showing GLR-dependent propagation of electrical signals and Ca^{2+} waves upon wounding in *M. polymorpha*. Moreover, our histological analyses have determined that Mp*GLR* is mostly expressed at the central part of the thallus encompassing the midrib. Transient expression studies showed that MpGLR localises to the ER and MVB/PVCs. This subcellular localisation is shared with vascular plants (Nguyen *et al.*, 2018), suggesting that the ER may have played an important role in regulating cytosolic Ca^{2+} levels along plant evolution.

Both GLR-dependent membrane depolarisations and $[Ca^{2+}]_{cyt}$ waves are the signature of systemic wound signalling that, however, does not result in gene reprogramming in distal, nondamaged tissues of the wounded *M. polymorpha* plants. Fossil record and molecular clock studies indicate that embryophytes (land plants) are monophyletically derived from green algae related to extant Charophyte (Delwiche & Cooper, 2015; Donoghue *et al.*, 2021; Bowman, 2022), that had already colonised subaerial habitats, with separation of bryophytes and tracheophytes occurring early upon land colonisation. The oldest fossils displaying the signs of herbivory are those of liverworts similar to extant ones, which in addition show the marks of local defensive responses (Labandeira *et al.*, 2014). Once on land, the evolution of a vascular tissue, among other traits, allowed for the more rapid distribution throughout the plant body of electrical signals and $[Ca^{2+}]_{cyt}$ transients that may have already been present in their algal predecessors. Indeed, under different stress conditions, extant charophytes display changes in membrane potential and $[Ca^{2+}]_{cyt}$ transient variations (Kisnieriene *et al.*, 2022), suggesting that membrane depolarisations and $[Ca^{2+}]_{cyt}$ variations may have occurred already in the common streptophyte ancestor in response to adverse conditions. Moreover, the vasculature also permitted the incorporation of chemical elicitors to the battery of danger signals. The nature of these chemical elicitors ultimately responsible for mounting the systemic responses may have diversified with the evolution of tracheophytes (Gao *et al.*, 2023).

Among those chemical elicitors identified, glutamate may play a role as a mediator activating GLR channels, both locally and at distal tissues, thus facilitating Ca^{2+} influx from the apoplast leading to $[Ca^{2+}]_{cyt}$ increases (Toyota *et al.*, 2018; Grenzi *et al.*, 2023). Remarkably, although $[Ca^{2+}]_{cyt}$ transients are observed in distal tissues of *M. polymorpha*, no systemic defence response occurs.

It has been suggested that vasculature is a character that liverworts lost during evolution, rather than being an acquisition along the expansion of tracheophytes (Harris *et al.*, 2022), while being maintained in some mosses for which advanced vascular functions have recently been uncovered (Brodribb *et al.*, 2020). If this intriguing hypothesis is correct, the presence of electrical signals and $[Ca^{2+}]_{cyt}$ transients upon wounding in *M. polymorpha* would suggest that they are part of an ancestral defence response whose functional systemic output as defence signalling could have been lost along the evolutionary disappearance of the vascular tissue. However, in the moss *Physcomitrella patens*, electrical signals triggered upon glutamate feeding or hydrogen peroxide application exhibit long-distance transmission while $[Ca^{2+}]_{cyt}$ transients are only local (Koselski *et al.*, 2020, 2023), suggesting that different combinations of local and systemic signals may have evolved.

The absence of vascular tissues in most bryophytes, whether by evolutionary loss or divergent evolution, has likely precluded the deployment of certain chemical elicitors of systemic defence signalling. Comparative analysis at the molecular level is indeed revealing that rewiring of ancient signalling pathways underlies many of the stress signalling pathways active in extant land plants (de Vries *et al.*, 2018; Fürst-Jansen *et al.*, 2020, and references therein). Thus, electrical signals and $[Ca^{2+}]_{cyt}$ transients are likely primordial danger signals that vascular plants recruited for the long-distance transmission and mounting of a systemic defence response to herbivory.

Acknowledgements

We thank Prof. Roberto Solano for providing WT plant material. We wish to thank Ms Soledad Montalbán and the Histology Facility at CNB-CSIC for the histological preparation of biological samples, and Mr Alberto Iniesta (Prof. Solano's laboratory) for help in designing CRISPR-Cas gRNA primers. We also thank Ms Aurore Chételat for excellent technical support. We are grateful to Prof. Roberto Solano and Dr Andrea Chini for fruitful discussions, and the critical reading of the manuscript. This work was funded by grants from the Spanish Ministry for Science and Innovation MCIN/AEI/10.13039/501100011033/FEDER 'Una manera de hacer Europa' (PID2021-122232NB-I00 to MS and PID2021-128078NB-I00 to ER) and from the Swiss National Science Foundation (310030_205203 and 31003A-175566 to EEF); PB-G was supported by a JAE-Intro fellowship (JAEINT_22_00306). MS, ER and JJSS are part of the Spanish Research Network EvoDevoSigNet (Grant RED2022-134917-T funded by the Spanish Ministry of Science and Innovation/Agencia Estatal de Investigación/10.13039/501100011033).

Competing interests

None declared.

Author contributions

MS, ER, EEF and JJS-S conceived and designed the experiments. MS, ER, JJS-S, AK, BL-G, MOD and PB-G performed the experiments. AMZ performed and JMG-M supervised oxylipin determination. ER supervised the molecular analyses. MS supervised *Marchantia polymorpha* transformation. JJS-S designed and wrote the manuscript. All authors read, gave critical feedback and approved the manuscript. MS and ER contributed equally to this work.

ORCID

Pavel Brito-Gutiérrez https://orcid.org/0009-0009-8179-8184
M. Otilia Delgadillo https://orcid.org/0000-0003-3788-3209
Edward E. Farmer https://orcid.org/0000-0002-6572-5024
José M. García-Mina https://orcid.org/0000-0001-6352-9612
Andrzej Kurenda https://orcid.org/0000-0001-8655-1046
Beatriz Larruy-García https://orcid.org/0009-0003-0579-935X
Enrique Rojo https://orcid.org/0000-0001-9886-2917
Jose J. Sánchez-Serrano https://orcid.org/0000-0002-4489-4785
Maite Sanmartín https://orcid.org/0000-0003-2038-6580
Ángel M. Zamarreño https://orcid.org/0000-0003-1966-0239

Data availability

RNA-Seq and Microarray data are available at NCBI Gene Expression Omnibus (GSE250353 https://www.ncbi.nlm.nih.gov/geo/query/acc.cgi?acc=GSE250353; GSE250354 https://www.ncbi.nlm.nih.gov/geo/query/acc.cgi?acc=GSE250354; GSE250478 https://www.ncbi.nlm.nih.gov/geo/query/acc.cgi?acc=GSE250478).

References

Althoff F, Kopischke S, Zobell O, Ide K, Ishizaki K, Kohchi T, Zachgo S. 2014. Comparison of the MpEF1α and CaMV35 promoters for application in *Marchantia polymorpha* overexpression studies. *Transgenic Research* **23**: 235–244.

Bowman JL. 2022. The origin of a land flora. *Nature Plants* **8**: 1352–1369.

Bowman JL, Arteaga-Vazquez M, Berger F, Briginshaw LN, Carella P, Aguilar-Cruz A, Davies KM, Dierschke T, Dolan L, Dorantes-Acosta AE *et al.* 2022. The renaissance and enlightenment of *Marchantia* as a model system. *Plant Cell* **34**: 3512–3542.

Bowman JL, Kohchi T, Yamato KT, Jenkins J, Shu S, Ishizaki K, Yamaoka S, Nishihama R, Nakamura Y, Berger F *et al.* 2017. Insights into land plant evolution garnered from the *Marchantia polymorpha* genome. *Cell* **171**: 287–304.e15.

Brodribb TJ, Carriquí M, Delzon S, McAdam SAM, Holbrook NM. 2020. Advanced vascular function discovered in a widespread moss. *Nature Plants* **6**: 273–279.

Browse J. 2009. Jasmonate passes muster: a receptor and targets for the defense hormone. *Annual Review of Plant Biology* **60**: 183–205.

Buatois LA, Davies NS, Gibling MR, Krapovickas V, Labandeira CC, MacNaughton RB, Mángano MG, Minter NJ, Shillito AP. 2022. The invasion of the land in deep time: integrating Paleozoic records of paleobiology, ichnology, sedimentology, and geomorphology. *Integrative and Comparative Biology* **62**: 297–331.

Chini A, Fonseca S, Chico JM, Fernández-Calvo P, Solano R. 2009. The ZIM domain mediates homo- and heteromeric interactions between Arabidopsis JAZ proteins. *The Plant Journal* **59**: 77–87.

Chini A, Fonseca S, Fernández G, Adie B, Chico JM, Lorenzo O, García-Casado G, López-Vidriero I, Lozano FM, Ponce MR *et al.* 2007. The JAZ family of repressors is the missing link in jasmonate signalling. *Nature* **448**: 666–671.

Chini A, Monte I, Zamarreño AM, García-Mina JM, Solano R. 2023. Evolution of the jasmonate ligands and their biosynthetic pathways. *New Phytologist* **238**: 2236–2246.

De Bortoli S, Teardo E, Szabò I, Morosinotto T, Alboresi A. 2016. Evolutionary insight into the ionotropic glutamate receptor superfamily of photosynthetic organisms. *Biophysical Chemistry* **218**: 14–26.

Delessert C, Wilson IW, Van Der Straeten D, Dennis ES, Dolferus R. 2004. Spatial and temporal analysis of the local response to wounding in *Arabidopsis* leaves. *Plant Molecular Biology* **55**: 165–181.

Delgadillo MO, Ruano G, Zouhar J, Sauer M, Shen J, Lazarova A, Sanmartín M, Lai LTF, Deng C, Wang P *et al.* 2020. MTV proteins unveil ER- and microtubule-associated compartments in the plant vacuolar trafficking pathway. *Proceedings of the National Academy of Sciences, USA* **117**: 9884–9895.

Delwiche CF, Cooper ED. 2015. The evolutionary origin of a terrestrial flora. *Current Biology* **25**: R899–R910.

Donoghue PCJ, Harrison CJ, Paps J, Schneider H. 2021. The evolutionary emergence of land plants. *Current Biology* **31**: R1281–R1298.

Farmer EE, Gao Y-Q, Lenzoni G, Wolfender J-L, Wu Q. 2020. Wound- and mechanostimulated electrical signals control hormone responses. *New Phytologist* **227**: 1037–1050.

Fürst-Jansen JMR, de Vries S, de Vries J. 2020. Evo-physio: on stress responses and the earliest land plants. *Journal of Experimental Botany* **71**: 3254–3269.

Gao Y-Q, Jimenez-Sandoval P, Tiwari S, Stolz S, Wang J, Glauser G, Santiago J, Farmer EE. 2023. Ricca's factors as mobile proteinaceous effectors of electrical signaling. *Cell* **186**: 1337–1351.

Gao Y-Q, Morin H, Marcourt L, Yang T-H, Wolfender J-L, Farmer EE. 2024. Chloride, glutathiones, and insect-derived elicitors introduced into the xylem trigger electrical signaling. *Plant Physiology* **194**: 1091–1103.

Gimenez-Ibañez S, Zamarreño AM, García-Mina JM, Solano R. 2019. An evolutionarily ancient immune system governs the interactions between *Pseudomonas syringae* and an early-diverging land plant lineage. *Current Biology* **29**: 2270–2281.e4.

Green TR, Ryan CA. 1972. Wound-induced proteinase inhibitor in plant leaves: a possible defense mechanism against insects. *Science* **175**: 776–777.

Grenzi M, Buratti S, Parmagnani AS, Aziz IA, Bernacka-Wojcik I, Resentini F, Simura J, Docula FG, Alfieri A, Luoni L *et al.* 2023. Long-distance turgor pressure changes induce local activation of plant glutamate receptor-like channels. *Current Biology* **33**: 1019–1035.

Harris BJ, Clark JW, Schrempf D, Szöllősi GJ, Donoghue PCJ, Hetherington AM, Williams TA. 2022. Divergent evolutionary trajectories of bryophytes and tracheophytes from a complex common ancestor of land plants. *Nature Ecology & Evolution* **6**: 1634–1643.

Hernick LV, Landing E, Bartowski KE. 2008. Earth's oldest liverworts—*Metzgeriothallus sharonae* sp. *nov.* from the Middle Devonian (Givetian) of eastern New York, USA. *Review of Palaeobotany and Palynology* **148**: 154–162.

Hilleary R, Gilroy S. 2018. Systemic signaling in response to wounding and pathogens. *Current Opinion in Plant Biology* **43**: 57–62.

Ishizaki K, Nishihama R, Ueda M, Inoue K, Ishida S, Nishimura Y, Shikanai T, Kohchi T. 2015. Development of gateway binary vector series with four different selection markers for the liverwort *Marchantia polymorpha*. *PLoS ONE* **10**: e0138876.

Kenrick P, Crane PR. 1997. The origin and early evolution of plants on land. *Nature* **389**: 33–39.

Kilian J, Whitehead D, Horak J, Wanke D, Weinl S, Batistic O, D'Angelo C, Bornberg-Bauer E, Kudla J, Harter K. 2007. The AtGenExpress global stress expression data set: protocols, evaluation and model data analysis of UV-B light, drought and cold stress responses. *The Plant Journal* **50**: 347–363.

Kimberlin AN, Holtsclaw RE, Zhang T, Mulaudzi T, Koo AJ. 2022. On the initiation of jasmonate biosynthesis in wounded leaves. *Plant Physiology* **189**: 1925–1942.

Kisnieriene V, Trębacz K, Pupkis V, Koselski M, Lapeikaite I. 2022. Evolution of long-distance signalling upon plant terrestrialization: comparison of action potentials in *Characean* algae and liverworts. *Annals of Botany* **130**: 457–475.

Kneeshaw S, Soriano G, Monte I, Hamberg M, Zamarreño ÁM, García-Mina JM, Franco-Zorrilla JM, Kato N, Ueda M, Rey-Stolle MF *et al.* 2022. Ligand diversity contributes to the full activation of the jasmonate pathway in *Marchantia polymorpha*. *Proceedings of the National Academy of Sciences, USA* **119**: e2202930119.

Kohchi T, Yamato KT, Ishizaki K, Yamaoka S, Nishihama R. 2021. Development and molecular genetics of *Marchantia polymorpha*. *Annual Review of Plant Biology* **72**: 677–702.

Koselski M, Hoernstein SNW, Wasko P, Reski R, Trebacz K. 2023. Long-distance electrical and Calcium signals evoked by hydrogen peroxide in *Physcomitrella*. *Plant & Cell Physiology* **64**: 880–892.

Koselski M, Pupkis V, Hashimoto K, Lapeikaite I, Hanaka A, Wasko P, Plukaite E, Kuchitsu K, Kisnieriene V, Trebacz K. 2021. Impact of mammalian two-pore channel inhibitors on long-distance electrical signals in the *Characean* Macroalga *Nitellopsis obtusa* and the early terrestrial liverwort *Marchantia polymorpha*. *Plants* **10**: 647.

Koselski M, Wasko P, Derylo K, Tchorzewski M, Trebacz K. 2020. Glutamate-induced electrical and calcium signals in the moss *Physcomitrella patens*. *Plant & Cell Physiology* **61**: 1807–1817.

Kubota A, Ishizaki K, Hosaka M, Kohchi T. 2013. Efficient *Agrobacterium*-mediated transformation of the liverwort *Marchantia polymorpha* using regenerating thalli. *Bioscience, Biotechnology and Biochemistry* **77**: 167–172.

Kupisz K, Dziubińska H, Trębacz K. 2017. Generation of action potential-type changes in response to darkening and illumination as indication of the plasma membrane proton pump status in *Marchantia polymorpha*. *Acta Physiologiae Plantarum* **39**: 82.

Kurenda A, Nguyen CT, Chételat A, Stolz S, Farmer EE. 2019. Insect-damaged *Arabidopsis* moves like wounded *Mimosa pudica*. *Proceedings of the National Academy of Sciences, USA* **116**: 26066–26071.

Labandeira CC, Tremblay SL, Bartowski KE, VanAller HL. 2014. Middle Devonian liverwort herbivory and antiherbivore defence. *New Phytologist* **202**: 247–258.

Labandeira CC, Wappler T. 2023. Arthropod and pathogen damage on fossil and modern plants: exploring the origins and evolution of herbivory on land. *Annual Review of Entomology* **68**: 341–361.

León J, Rojo E, Sánchez-Serrano JJ. 2001. Wound signalling in plants. *Journal of Experimental Botany* **52**: 1–9.

Liang Y, Heyman J, Xiang Y, Vandendriessche W, Canher B, Goeminne G, De Veylder L. 2022. The wound-activated ERF15 transcription factor drives *Marchantia polymorpha* regeneration by activating an oxylipin biosynthesis feedback loop. *Science Advances* **8**: eabo7737.

Monte I, Franco-Zorrilla JM, García-Casado G, Zamarreño AM, García-Mina JM, Nishihama R, Kohchi T, Solano R. 2019. A single JAZ repressor controls the jasmonate pathway in *Marchantia polymorpha*. *Molecular Plant* **12**: 185–198.

Monte I, Ishida S, Zamarreño AM, Hamberg M, Franco-Zorrilla JM, García-Casado G, Gouhier-Darimont C, Reymond P, Takahashi K, García-Mina JM *et al.* 2018. Ligand-receptor co-evolution shaped the jasmonate pathway in land plants. *Nature Chemical Biology* **14**: 480–488.

Morris JL, Puttick MN, Clark JW, Edwards D, Kenrick P, Pressel S, Wellman CH, Yang Z, Schneider H, Donoghue PCJ. 2018. The timescale of early land plant evolution. *Proceedings of the National Academy, USA* **115**: E2274–E2283.

Mousavi SAR, Chauvin A, Pascaud F, Kellenberger S, Farmer EE. 2013. GLUTAMATE RECEPTOR-LIKE genes mediate leaf-to-leaf wound signalling. *Nature* **500**: 422–426.

Nakagawa T, Kurose T, Hino T, Tanaka K, Kawamukai M, Niwa Y, Toyooka K, Matsuoka K, Jinbo T, Kimura T. 2007. Development of series of gateway binary vectors, pGWBs, for realizing efficient construction of fusion genes for plant transformation. *Journal of Bioscience and Bioengineering* **104**: 34–41.

Nguyen CT, Kurenda A, Stolz S, Chételat A, Farmer EE. 2018. Identification of cell populations necessary for leaf-to-leaf electrical signaling in a wounded plant. *Proceedings of the National Academy of Sciences, USA* **115**: 10178–10183.

Puttick MN, Morris JL, Williams TA, Cox CJ, Edwards D, Kenrick P, Pressel S, Wellman CH, Schneider H, Pisani D *et al.* 2018. The interrelationships of land plants and the nature of the ancestral embryophyte. *Current Biology* **28**: 733–745.e2.

Sanmartín M, Sauer M, Muñoz A, Zouhar J, Ordóñez A, Van De Ven WTG, Caro E, De La Paz SM, Raikhel NV, Gutiérrez C *et al.* 2011. A molecular switch for initiating cell differentiation in *Arabidopsis*. *Current Biology* **21**: 999–1008.

Schilmiller A, Howe G. 2005. Systemic signaling in the wound response. *Current Opinion Plant Biology* **8**: 369–377.

Shimamura M. 2016. *Marchantia polymorpha*: taxonomy, phylogeny and morphology of a model system. *Plant and Cell Physiology* **57**: 230–256.

Thines B, Katsir L, Melotto M, Niu Y, Mandaokar A, Liu G, Nomura K, He SY, Howe GA, Browse J. 2007. JAZ repressor proteins are targets of the SCF(COI1) complex during jasmonate signalling. *Nature* **448**: 661–665.

Tian L, Hires SA, Mao T, Huber D, Chiappe ME, Chalasani SH, Petreanu L, Akerboom J, McKinney SA, Schreiter ER *et al.* 2009. Imaging neural activity in worms, flies and mice with improved GCaMP calcium indicators. *Nature Methods* **6**: 875–881.

Tihelka E, Howard RJ, Cai C, Lozano-Fernandez J. 2022. Was there a Cambrian explosion on land? The case of *Arthropod* terrestrialization. *Biology* **11**: 1516.

Titarenko E, Rojo E, León J, Sánchez-Serrano JJ. 1997. Jasmonic acid-dependent and -independent signaling pathways control wound-induced gene activation in *Arabidopsis thaliana*. *Plant Physiology* **115**: 817–826.

Toyota M, Spencer D, Sawai-Toyota S, Jiaqi W, Zhang T, Koo AJ, Howe GA, Gilroy S. 2018. Glutamate triggers long-distance, calcium-based plant defense signaling. *Science* **361**: 1112–1115.

de Vries J, Archibald JM. 2018. Plant evolution: landmarks on the path to terrestrial life. *New Phytologist* **218**: 1428–1434.

de Vries J, Curtis BA, Gould SB, Archibald JM. 2018. Embryophyte stress signaling evolved in the algal progenitors of land plants. *Proceedings of the National Academy of Sciences, USA* **115**: E3471–E3480.

Wang P-H, Lee C-E, Lin Y-S, Lee M-H, Chen P-Y, Chang H-C, Chang I-F. 2019. The glutamate receptor-like protein GLR3.7 interacts with 14-3-3ω and participates in salt stress response in *Arabidopsis thaliana*. *Frontiers in Plant Science* **10**: 1169.

Wasternack C, Hause B. 2013. Jasmonates: biosynthesis, perception, signal transduction and action in plant stress response, growth and development. An update to the 2007 review in Annals of Botany. *Annals of Botany* **111**: 1021–1058.

Watanabe K, Hashimoto K, Hasegawa K, Shindo H, Tsuruda Y, Kupisz K, Koselski M, Wasko P, Trebacz K, Kuchitsu K. 2024. Rapid propagation of Ca^{2+} waves and electrical signals in a liverwort *Marchantia polymorpha*. *Plant & Cell Physiology* **65**: 660–670.

Wellman CH, Osterloff PL, Mohiuddin U. 2003. Fragments of the earliest land plants. *Nature* **425**: 282–285.

Wickett NJ, Mirarab S, Nguyen N, Warnow T, Carpenter E, Matasci N, Ayyampalayam S, Barker MS, Burleigh JG, Gitzendanner MA *et al.* 2014. Phylotranscriptomic analysis of the origin and early diversification of land plants. *Proceedings of the National Academy of Sciences, USA* **111**: E4859–E4868.

Woudenberg S, Renema J, Tomescu AMF, De Rybel B, Weijers D. 2022. Deep origin and gradual evolution of transporting tissues: perspectives from across the land plants. *Plant Physiology* **190**: 85–99.

Wudick MM, Michard E, Oliveira Nunes C, Feijó JA. 2018. Comparing plant and animal glutamate receptors: common traits but different fates? *Journal of Experimental Botany* **69**: 4151–4163.

Yan C, Gao Q, Yang M, Shao Q, Xu X, Zhang Y, Luan S. 2024. Ca^{2+}/Calmodulin- mediated desensitization of glutamate receptors shapes plant systemic wound signalling and anti-herbivore defence. *Nature Plants* **10**: 145–160.

Zheng Y, Luo L, Wei J, Chen Q, Yang Y, Hu X, Kong X. 2018. The glutamate receptors AtGLR1.2 and AtGLR1.3 increase cold tolerance by regulating jasmonate signaling in *Arabidopsis thaliana*. *Biochemical and Biophysical Research Communications* **506**: 895–900.

See also the Commentary on this article by Beraldo & Alboresi, **244**: 743–745.

Supporting Information

Additional Supporting Information may be found online in the Supporting Information section at the end of the article.

Fig. S1 Schematic representation of the mechanical wounding procedure of *Marchantia polymorpha* and the tissues collected for oxylipin profiling and gene expression analysis.

Fig. S2 Genome editing of MpGLR to generate Mp*glr* loss-of-function mutants in *Marchantia polymorpha*.

Fig. S3 Growth and development of *Marchantia polymorpha* L47, L48, Mp*glr-7* and Mp*glr-9* plants.

Fig. S4 Wound-induced $[Ca^{2+}]_{cyt}$ transients in soil-grown *Marchantia polymorpha* WT and Mp*glr* mutant plants.

Table S1 Primer sequences used in this study.

Table S2 Transcriptional profiling of the local and systemic wound response in the *Marchantia polymorpha* Mp*glr* mutants and the corresponding L47 and L48 parental lines.

Table S3 Transcriptional profiling of the local and systemic wound response in *Marchantia polymorpha* Tak-1 wild-type plants.

Table S4 Oxylipin accumulation in *Marchantia polymorpha* thalli after wounding.

Video S1 Systemic transmission of electrical signals in *Marchantia polymorpha* wild-type Tak-1 plants upon wounding.

Video S2 Systemic transmission of electrical and Ca^{2+} signals in *Marchantia polymorpha* L47 calcium sensor line upon wounding.

Video S3 Mechanical wounding induces distal $[Ca^{2+}]_{cyt}$ increases in *Marchantia polymorpha*.

Video S4 Systemic transmission of electrical and Ca^{2+} signals is blocked in *Marchantia polymorpha* Mp*glr* mutants.

Please note: Wiley is not responsible for the content or functionality of any Supporting Information supplied by the authors. Any queries (other than missing material) should be directed to the *New Phytologist* Central Office.